

An evaluation of damage development for CFRTP by conventional tows and spread tows using acoustic emission

Takayuki Kinoshita^{1*}, Tetsusei Kurashiki¹, Kazutaka Mukoyama¹,
Koushu Hanaki¹, Masaru Zako¹, Xingsheng Li¹, Stepan V. Lomov²

¹Graduate Student of Eng., Osaka University, Osaka, 565-0871, Japan

² Department of Metallurgy and Materials Engineering, KU Leuven, Kasteelpark
Arenberg 44, B-3001 Leuven, Belgium

* kinoshita-t@mit.eng.osaka-u.ac.jp

Abstract. Comparison of damage development of textile composites made by combination of two resin (Polyamide and Epoxy) and two kinds of fiber bundles (conventional tows and spread tows) is carried out. The quasi-static tensile tests were carried out with using DIC (digital image correlation) system to estimate the full field strain and AE (acoustic emission) sensors for measurement of the acoustic emission features. The CFRTP specimens were also investigated with optical microscope to clarify the difference of damage. Fig.1 shows characteristic damage of each CFRTP. The fiber debonding and delamination were shown in CF(with spread tows)/PA composites and the damage in weft yarn covered a wide range of test specimens. It is suggested that these features of damage were influenced with effect of fiber opening. This may also be explained by AE events. In weft yarn of CF(with conventional tows)/PA composites, we observed not only transverse crack but also clack which propagated parallel to loading direction. This type of crack was not found in other thermoplastic carbon composites such as CF/PPS described in the literature. From these results, we conclude that the damage development of textile composites is sensitive to the form of fiber bundles and the properties of the matrix.

1. Introduction

Fiber reinforced plastic (FRP) is superior in specific strength, specific rigidity, and high flexibility in material design. Therefore, FRP is used in a wide range of fields, such as aircraft, aerospace and automobile where both light weighting and high strength are required. In particular, it is expected that carbon fiber reinforced thermoplastic (CFRTP) which contains matrix having high formability and high recyclability plays an important role in the composite material market from the environmental point of view. However, it is difficult to impregnate fiber bundles with thermoplastic because of its polymer structure. The focus of this paper is the comparison of damage development of textile composites with two different resin – Polyamide as thermoplastics and Epoxy as thermoset plastics, with two different fiber bundles – conventional tows and spread tows. Spread tows are very thin and wide tows. They are useful for preventing cracks caused by resin shortage in fiber bundles because it is easier to impregnate thin fiber bundles with resin.

In order to compare the damage development, acoustic emission (AE) registration and digital image correlation (DIC) system is used to obtain full field strain mapping during quasi-static tensile tests. After that, the damage pattern is investigated with an optical microscope.



2. Experimental setup

2.1. Test pieces

Specimens for tensile test were prepared referring to a part of the JIS K 7161: total length 250mm, gage length 150mm, width 30mm. With regard to PA6/CF_Spread specimen, the width is 50mm to take into account the periodicity of fiber bundles because the width of spread tows is approximately 20mm. The 50×30 mm tabs for specimens with conventional tows and 50×50 mm tabs for specimens with spread tows are attached with epoxy glue to the specimen ends to avoid failure during test in the grips of the testing machine. Measurements of the number of plies, thickness and fiber volume fraction (V_f) are listed in Table 1(a). The mechanical properties of Epoxy and PA6 are shown in Table 1(b).

Table 1. Material properties

| | Epoxy/CF | PA6/CF | PA6/CF_Spread |
|-----------------------------|-----------|-----------|---------------|
| (a) | | | |
| Number of plies | 10 | 10 | 19 |
| V_f (%) | 50.9± | 51.1± | 50.9± |
| Thickness (mm) | 1.95±0.05 | 2.08±0.04 | 1.79±0.03 |
| | Epoxy | PA6 | |
| (b) | | | |
| Density (g/cm^3) | 1.40 | 1.13 | |
| Tensile strength (MPa) | 80.6 | 80.0 | |
| Elastic modulus (GPa) | 3.18 | 2.80 | |

2.2. Test procedures

Tensile tests were performed using tensile testing equipment (INSTRON 4505 with a load cell of 100kN), and the crosshead speed was 1mm/min. Five specimens were prepared for each test. In order to obtain full field strain mapping, images of all specimens were acquired using LIMESS system. The images post-processing allowed the measurement of the full field strain on the external surface of the specimen by the DIC. Two AE sensors are attached to a specimen with a distance between their centers 100mm. The amplitude of 100 dB is a saturation limit and the threshold of 40 dB is set for noise reduction.

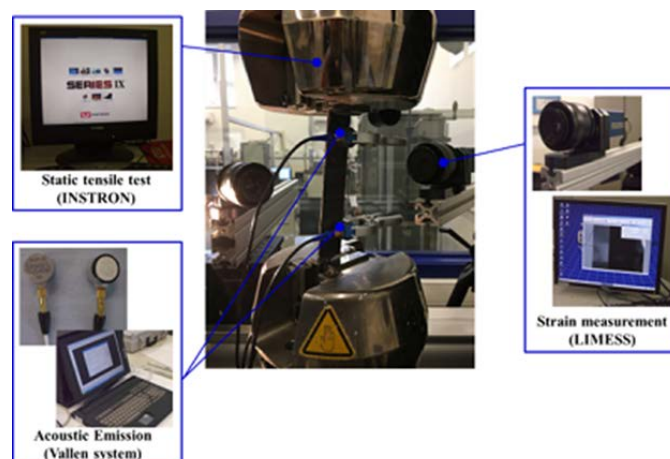


Figure 1. Test set-up

To investigate the damage patterns, samples for optical microscopy observation were prepared. The samples are cut to 20×15 mm from the center of the sample using diamond saw and then they are embedded in the plastic sample holder. Finally, they are polished by the automatic polishing machine.

Polishing was done in steps with different gauges of grinding paper, 3 μm diamond suspension and 1 μm diamond suspension.

3. Result of tensile test

3.1. Comparison of PA6/CF and Epoxy/CF

The average values, standard deviations and coefficient of variation (CV) of mechanical properties of the PA6/CF and Epoxy/CF composites in the warp direction were given in table 2. The Young's modulus was calculated by the slope of the stress-strain curves in the 0.1 to 0.3% strain region. Specimens were loaded up to failure.

Table 2. Tensile properties in the warp direction

| | PA6/CF | | | Epoxy/CF | | |
|-----------------------------|---------|-----------|------|----------|-----------|------|
| | Average | Std. dev. | CV | Average | Std. dev. | CV |
| Ultimate tensile strain (%) | 1.52 | 0.09 | 0.06 | 1.85 | 0.24 | 0.13 |
| Tensile strength (MPa) | 636 | 43.2 | 0.07 | 872 | 67.0 | 0.08 |
| Young's modulus (GPa) | 54.2 | 3.68 | 0.07 | 73.8 | 8.21 | 0.11 |

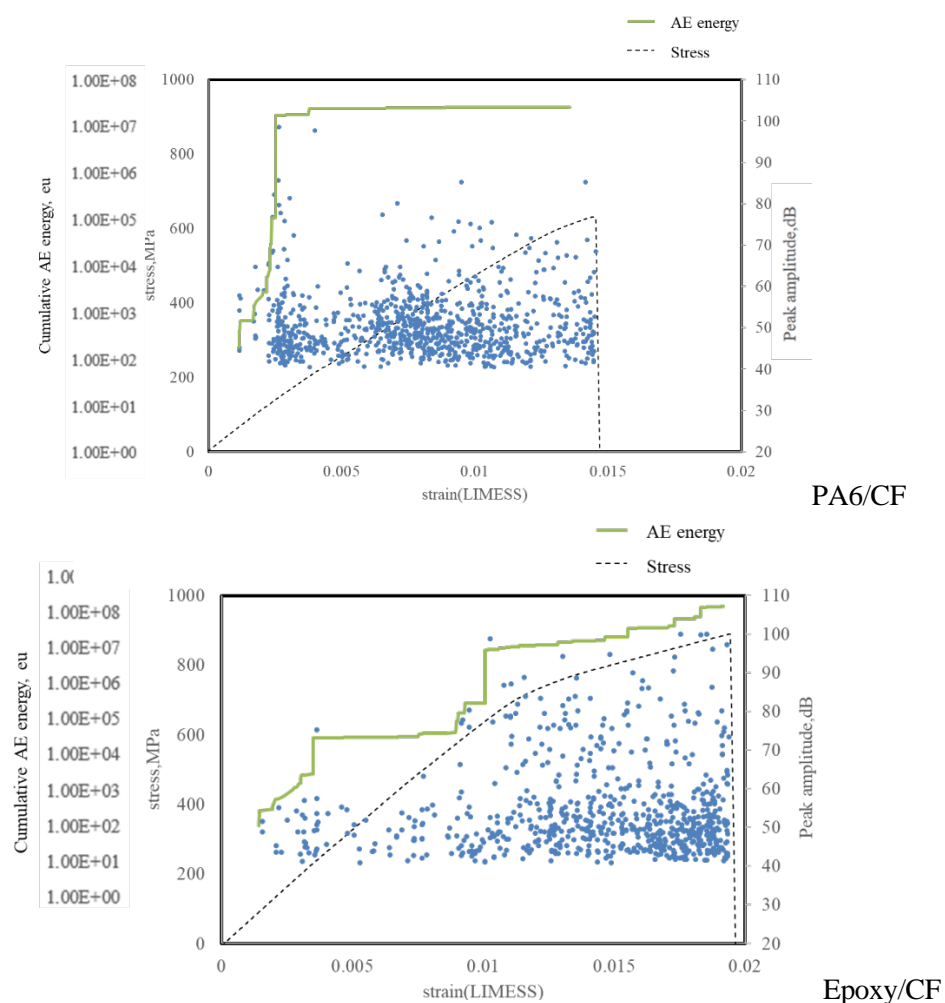


Figure 2. Representative cumulative AE energy, peak amplitude and stress-strain curve

Cumulative AE energy and peak amplitude are shown in Figure 2 for representative specimen, together with stress-strain curve. From the cumulative AE energy curve, damage initiation and development in PA6/CF composite is earlier than epoxy one. These initial damage may affect ultimate tensile strain and tensile strength. Figure 3 shows the characteristic damage patterns of each specimen. The initial damage in Epoxy/CF composite appears in the form of transverse cracks inside the yarns. It corresponds to the initial AE events with low amplitude. On the other hand, there are cracks parallel to loading direction inside weft yarns in PA6/CF composite. It could be consequence of the resin shortage in fiber bundles or the thermal residual stresses accumulated during manufacturing.

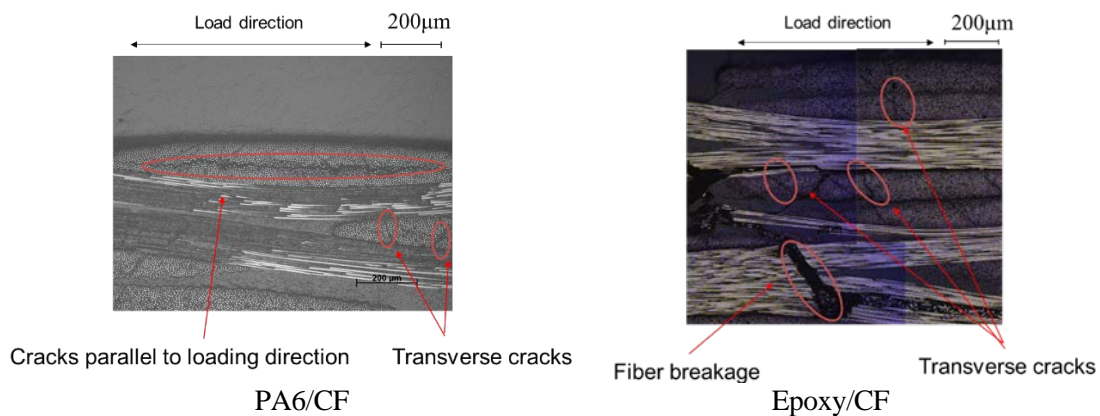


Figure 3. Characteristic damage pattern after tensile tests

3.2. Result of PA6/CF with spread tows

The average values, standard deviations and coefficient of variation (CV) of mechanical properties of the PA6/CF with spread tows in the warp direction are given in Table 3. It shows fiber opening brings remarkable increase in ultimate tensile strain. According to the observation result on specimen after failure, the specimen after failure, the reasons for this is large inter-ply delaminations.

Table 3. Tensile properties in the warp direction

| | PA6/CF_Spread | | |
|-----------------------------|---------------|-----------|------|
| | Average | Std. dev. | CV |
| Ultimate tensile strain (%) | 3.00 | 0.66 | 0.22 |
| Tensile strength (MPa) | 768 | 83.1 | 0.11 |
| Young modulus (GPa) | 51.8 | 6.16 | 0.12 |

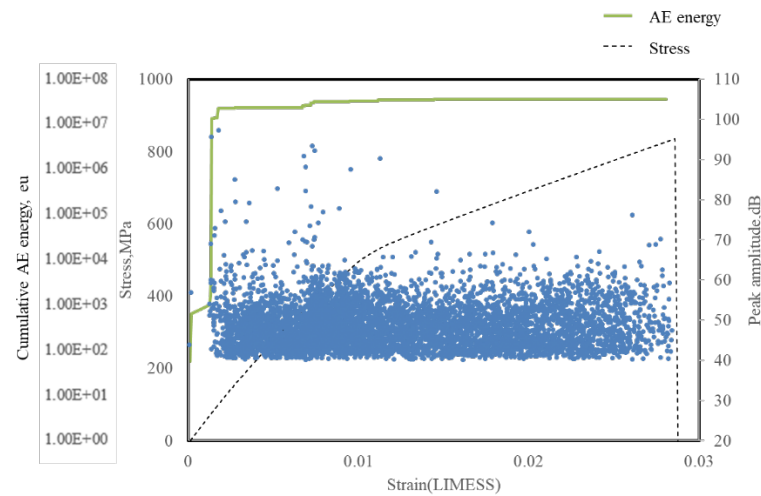


Figure 4. Representative cumulative AE energy, peak amplitude and stress-strain curve

Cumulative AE energy and peak amplitude are shown in Figure 4 for representative specimen with stress-strain curve. The shape of cumulative AE energy curve is similar to the curve of PA6/CF with conventional tows. On the other hand, the cumulative AE energy saturates earlier and the low amplitude events are corrected continuously. Figure 5 shows the characteristic damage patterns of PA6/CF with spread tows. Micro-debondings at the fiber-matrix interface and inter-ply delamination were appeared. However, there are not cracks parallel to loading direction inside weft yarns as observed in PA6/CF with conventional tows specimen. This phenomenon is effected by the spread tows which are superior in impregnation performance.

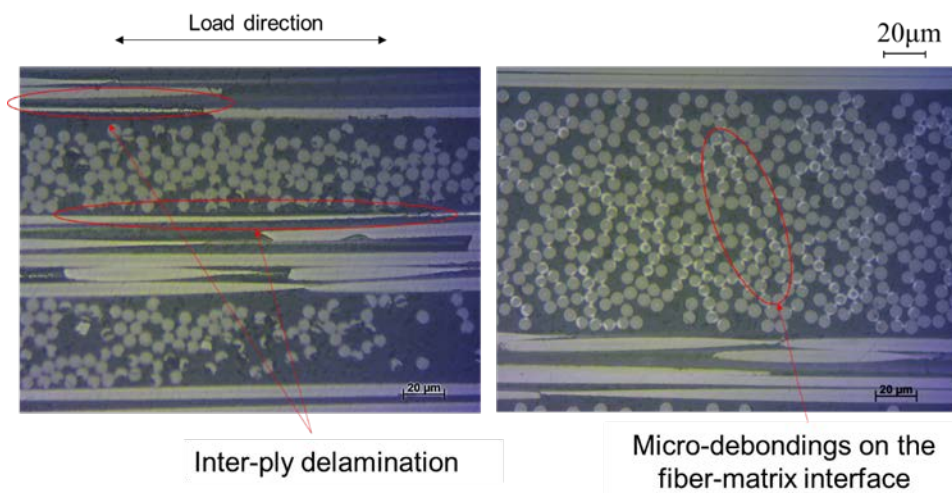


Figure 5. Characteristic damage pattern after tensile tests

4. Damage development analysis

As the damage observations were made on failure samples, FE analysis was carried out to observe damage development of PA6/CF and Epoxy/CF. The FE model is shown in Figure 6 and periodic boundary condition is applied to nodes on all plane of FE model. In this study, Hoffman law is used as failure criterion for elements. It is useful to take anisotropy damage mode into account. The mechanical

properties of fiber bundles are calculated from reinforcement fiber (TC-33) and each resin, using Chamis law and Rosen law. Damage development analysis imparting a strain of 0.1% step is carried out.

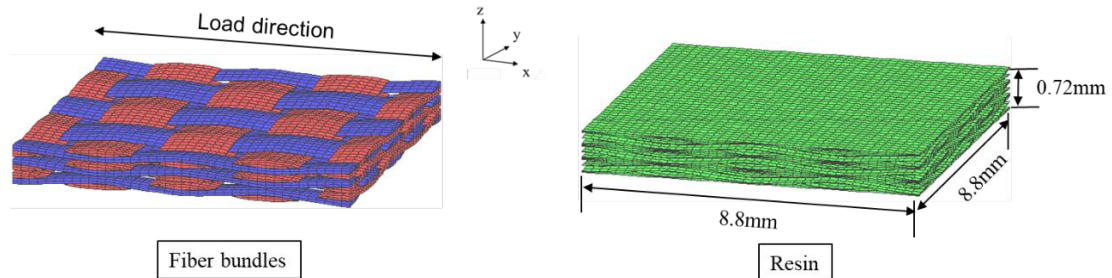


Figure 6. FE model of plain woven fabric

The damage development in fiber bundles of each sample is shown in Figure 7. In this case, damage mode T means transverse crack by normal stress component of transversal direction, mode ZL means delamination by shear stress component of in-plane direction and mode L means fiber breakage by normal stress component of longitudinal direction. Regarding to PA6/CF model, the area of initial damage is much larger than that of Epoxy/CF model. It is considered to be the reason why the difference of AE feature at low strain level appeared. Just before fracture, local delamination and fiber breakage appeared in Epoxy/CF model. As for PA6/CF model, a lot of delaminations in longitudinal yarns by shear stress were observed due to elongation of Polyamide.

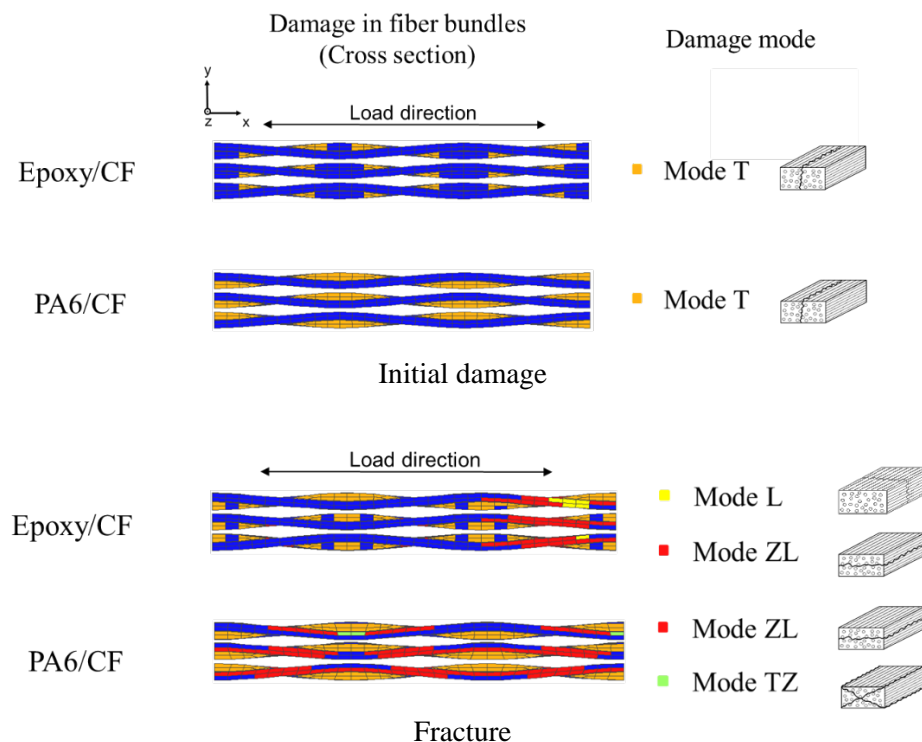


Figure 7. Damage state of each model

5. Conclusions

Table 4 shows a summary table of damage state for all specimens. The study concludes that the performance of textile composites were highly sensitive to the performance of the matrix such as impregnation characteristics. More specifically, a significant difference in damage development was found in PA6/CF, PA6/CF_Spread and Epoxy/CF composites as indicated by AE data and crack observations. Tensile properties in warp direction were found to be dependent on the matrix behaviour.

Table 4. Characteristics of damage state

| | Epoxy/CF | PA6/CF | PA6/CF_Spread |
|--|----------|--------|---------------|
| Transverse cracks | ○ | ○ | △ |
| Micro-debondings on the fiber-matrix interface | △ | × | ○ |
| Cracks parallel to warp direction | × | ○ | × |
| Inter-ply delamination | ○ | × | ○ |

Acknowledgments

The authors would like to express our thanks to Maruhachi Co. Ltd., Japan for the cooperation.

References

- [1] Sergey G Ivanov, Dries Beyens, et al. Damage development in woven carbon fibre thermoplastic laminates with PPS and PEEK matrices: A comparative study. *Journal of Composite Materials* 2017, Vol. 51(5) 637–647. DOI: 10.1177/0021998316653460.
- [2] Valter Carvelli. Acoustic emission and damage mode correlation in textile reinforced PPS composites. *Composite Structures* 2017, Vol. 163 399–409.
- [3] M. Zako. Finite element analysis of damaged woven fabric composite materials. *Composite Science and Technology* 2003, Vol. 63 507–516
- [4] Yuzo Fujita, Effect of Micro Structure on Mechanical Properties of Woven Fabric Composite, *Safety, Reliability and Risk of Structures, Infrastructures and Engineering Systems* 2009, Vol.10 3477-3484